Appl Phys B (2009) 94: 503–511
DOI 10.1007/s00340-008-3248-3

Applied Physics B
Lasers and Optics

Structure and NLO property relationship in a novel chalcone co-crystal

H.J. Ravindra · K. Chandrashekaran · W.T.A. Harrison · S.M. Dharmaprakash

Received: 8 August 2008 / Published online: 23 October 2008

Abstract Single crystals of a chalcone co-crystal ($C_{18}H_{19}NO_4/C_{17}H_{16}NO_3Br$; 0.972/0.028) have been grown by slow evaporation from solution. The powder second harmonic generation (SHG) efficiency of this chalcone co-crystal is 7 times that of urea. The dependence of second harmonic (SH) intensity on particle size revealed the existence of phase matching direction in this crystal. The large SHG efficiency observed is mainly due to the unidirectional alignment of molecular dipoles, in which the dipole moment of each molecule adds to establish a net polarization. The weak N–H···O hydrogen-bond interactions help to stabilize the noncentrosymmetric crystal packing and also contribute partly to the SHG. The better thermal stability, transparency and high laser damage resistance (>1.5 GW cm^{-2} at 532 nm, 8 ns) of this chalcone co-crystal indicate that it is a promising material for frequency doubling of diode lasers down to 470 nm. This molecule also shows a third-order NLO response and good optical limiting property of 8 ns laser pulses at 532 nm. The mechanism for optical limiting in this chalcone was attributed to two-photon induced excited state absorption that leads to reverse saturable absorption. The structure–property relationship in this chalcone and related compounds is discussed based on the experimental results and semiempherical hyperpolarizability calculations.

PACS 42.65.An · 42.70.Nq

1 Introduction

Organic NLO materials have attracted considerable interest in the past three decades due to their potential application in optical switches, modulators, optical limiters, and optical data storage [1, 2]. Organic materials are of particular interest because of their versatile synthetic flexibility that offers one to fine tune the optical properties at molecular level. Moreover, the optical nonlinearity in this class of materials is electronic in origin and hence exhibits an ultra fast response. The microscopic first hyperpolarizability (β) of NLO chromophores at molecular level can be maximized by optimizing the extent of charge transfer across the molecule. The strongest push–pull effect occurs when the strong electron donors' and acceptors' groups are separated by an extended π-conjugated bridge. Molecules exhibiting these structural features also tend to have a high molecular dipole moment. However, a high molecular dipole moment generally forces the molecules to pack centrosymmetrically in a crystal lattice since the dipoles in adjacent molecules will tend to align in an anti-parallel fashion. For second-order NLO process such as second harmonic generation (SHG) one requires crystallographic noncentrosymmetry for a nonzero SHG ($\chi^2 \neq 0$). To maximize the macroscopic response (χ^2), it is necessary to have a head-to-tail alignment

H.J. Ravindra (✉) · S.M. Dharmaprakash
Department of Physics, Mangalore University, Mangalagangotri 574 199, Karnataka, India
e-mail: ravi_23911@rediffmail.com
Fax: +91-082-42287367

K. Chandrashekaran
Lasers and Nonlinear Optics Lab, Department of Science and Humanities, National Institute of Technology, Calicut 673 601, Kerala, India

W.T.A. Harrison
Department of Chemistry, University of Aberdeen, Meston Walk, Aberdeen AB24 3UE, Scotland

of molecules connected through strong intermolecular hydrogen bond interactions in the solid state, and such molecular crystals usually exhibit good phase-matching characteristics.

Chalcones are a family of cross conjugated NLO chromophores that exhibit good SHG efficiency and transparency [3–6]. In recent years, co-crystals formed by two or more crystallizing components have gained the attention of researchers [7, 8]. By suitably selecting the molecular components, it is possible to fine tune the physico-chemical properties of co-crystals [9, 10]. The co-crystals have been proven successful as functional materials with applications in molecular electronics and optical applications [11, 12]. To prepare such co-crystals, grinding methods (grinding in the presence of a small amount of solvent) and solvent evaporation techniques have been employed [13–15]. Several donor-substituted co-crystals of chalcones have been prepared and the crystal structures have been reported [16–18]. The co-crystal of chalcone under present investigation crystallized in a noncentrosymmetric space group [19] and exhibited powder SHG efficiency 7 times greater than that of urea. Though these co-crystals of chalcones were accidentally obtained, they have significance for molecular engineering of an efficient SHG material with superior phase matching property (present study). In this article, we present our systematic studies on the structure and NLO property relationship in chalcone co-crystal ($C_{18}H_{19}NO_4/C_{17}H_{16}NO_3Br$; 0.972/0.028).

2 Experimental

The molecule 1-(4-aminophenyl)-3-(3, 4, 5-trimethoxyphenyl)prop-2-en-1-one (APTP) was synthesized using the standard procedure described in the literature [20]. The 4-amino acetophenone and 3, 4, 5-trimethoxybenzaldehyde used for synthesis are of analytical reagent (AR) grade. The compound was prepared by a Claisen–Schimidt condensation reaction and was purified by recrystallization process using acetone solvent. The purified compound melts in the temperature range of 161–163°C.

The choice of solvent in the solution growth technique often plays a vital role in single crystal growth of organic materials. We selected acetone as solvent for growing single crystals of this chalcone as its solubility was better compared with that in methanol and ethanol and a saturated solution was prepared. The solution temperature was raised by 5°C to get a homogeneous mixture of solution, which was filtered. Slow evaporation at ambient temperature resulted in the formation of multiple crystals with no well defined morphology, having maximum crystal size of 2 mm × 1 mm × 0.2 mm in 3 days. The grown crystals are transparent, non-hygroscopic, and are elongated along the crystallographic *c*-axis.

The size of the crystal obtained in the present case is sufficient to confirm the existence of a phase matching direction by the Kurtz powder SHG technique [21], which was measured relative to urea. A Nd:YAG laser operating at $\lambda = 1064$ nm with a pulse width of 8 ns and an energy of 0.27 mJ/pulse was used as the light source and a 10-cm focal length lens was used to focus the beam onto the sample. The scattered SH signal along with the scattered fundamental radiation was collected by a lens having longer focal length. The fundamental radiation was filtered using a Czerny–Turner type monochromator. The SH signal was then amplified using a photomultiplier tube (Hamamatsu R-2059) and displayed on a storage oscilloscope. The co-crystal and reference urea crystals pulverized to have particle size less than 125 μm were used in the relative SHG study. By fixing the fundamental laser energy constant, the relative SH signals of urea and chalcone were reliably measured.

To study the third-order NLO properties, the single beam Z-scan technique [22] was employed, which readily gives the magnitude and sign of the nonlinearity. The experiment was performed with 8 ns pulses at 532 nm generated from a Q-switched Nd:YAG laser. The spatial profiles of the optical pulses were nearly Gaussian. A lens of focal length 25 cm was used to focus the laser beam into a 1-mm quartz cuvette. The resulting beam waist radius at the focus was 19 μm, corresponding to a Rayleigh length of 2.15 mm. The Z-scan data were collected in a single-shot mode with the incident and transmitted laser pulse energies measured simultaneously by two pyroelectric energy detectors (Laser Probe, Rj-7620). For measuring the refractive nonlinear property, an aperture was placed in front of the detector and the transmittance was recorded as a function of the sample position on the Z-axis (closed aperture Z-scan). For measuring the nonlinear absorption, the sample transmittance was measured without the aperture as a function of sample position (open aperture Z-scan). The optical limiting measurements were carried out when the sample was at the focal point by varying the input energy and recording the output energy without placing an aperture in front of the detector.

3 Characterization

The as-grown crystals were characterized by elemental analysis (Vario EL III carbon hydrogen nitrogen sulfur analyzer), FT IR spectroscopy (Shimadzu 8700) and single crystal X-ray diffraction (Bruker SMART1000 CCD single crystal X-ray diffractometer).

Elemental analysis The measured percentage composition of the co-crystal is C 68.51% H 5.98% and N 4.43%, in good agreement with the calculated molecular formula (C 68.55%, H 6.05% and N 4.44%).

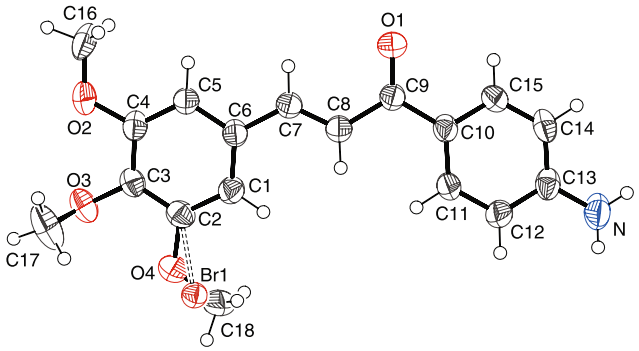

Fig. 1 The molecular structure of chalcone co-crystal (APTP/APBDP)

Table 1 Single Crystal Data of the APTP/APBDP co-crystal

Formula	0.972(C18 H19 N O4), 0.028(C17 H16 Br N O3)
Formula Weight	314.81
Crystal System	Monoclinic
Space group	*Pn*
a	4.2227 (4) Å
b	12.2001 (12) Å
c	15.4865 (16) Å
β	97.506 (2)°
V	790.99 (14) Å^3
Z	2
Density *D*	1.321 kg m^{-3}

FTIR spectral analysis The FTIR spectrum was collected in the spectral range of 400–4000 cm^{-1}, where the sample was in the KBr phase. υ(NH2) 3300–3500, υ(C–N) 1356.8, υ(arom C–H) 3100–3000, υ(asy & sym CH_3) 2937 & 2835, υ(C=O) 1631, υ(arom C=C) 1587, υ(C=C) 1506, υ(CH_3–O) 1454, and υ(C–Br) 820 cm^{-1}.

Single crystal X-ray diffraction A single crystal X-ray diffraction study of this chalcone was carried out to understand the structure and NLO property relationship. The detailed structure analysis can be found in our earlier publication on this crystal [19]. This chalcone crystallizes in noncentrosymmetric crystal structure and the molecular structure is shown in Fig. 1. The unit cell parameters determined are tabulated in Table 1. The presence of bromine component of chalcone in the grown co-crystal and also in the starting material (3, 4, 5-trimethoxybenzaldehyde) was confirmed by performing the halogen test [20].

4 Results and discussion

Our attempt to synthesize 1-(4-aminophenyl)-3-(3, 4, 5-trimethoxyphenyl)prop-2-en-1-one (APTP) also resulted in the formation of 1-(4-aminophenyl)-3-(3-bromo-4, 5-dimethoxyphenyl)prop-2-en-1-one (APBDP) due to the presence of an impurity of 3-bromo-4, 5-dimethoxybenzaldehyde in the 3, 4, 5-trimethoxybenzaldehyde starting material. During the crystallization process, the APBDP co-crystallizes with the APTP in noncentrosymmetric space group as established in our earlier study [19]. All the atoms are superimposed in the crystal, except for one of the methoxy group (O4/C18/H18a/H18b/H18c) in APTP and one bromine atom (Br1) in APBDP. We repeated the synthesis of the target molecule APTP from the same starting material and the crystal growth was carried out by maintaining the same experimental condition to check the reproducibility of the formation of this co-crystal and obtained similar results. However, it is interesting here to note that none of the co-crystals of chalcones reported in the literature possess a noncentrosymmetric structure, which is an essential requirement for a material to exhibit SHG.

The powder SHG efficiency of this co-crystal is 7 times that of urea (or 7 × U) for a similar range of particle sizes (<125 μm). This co-crystal has a higher SHG efficiency than *p*-chlorodibenzylideneacetone (4.5 × U) [3], 1, 3-bis(4-bromophenyl)prop-2-en-1-one (5.2 × U), 3-[4-(dimethylamino)phenyl]-1-(4-methoxyphenyl)prop-2-en-1-one (4 × U), 3-[4-(diethylamino)phenyl]-1-(4-methoxyphenyl)prop-2-en-1-one (∼2 × U), and a comparable SHG efficiency with that of 3-(4-bromophenyl)-1-phenylprop-2-en-1-one (7 × U) [23].

The existence of a phase matching direction in the crystal facilitates high SHG conversion efficiency at the phase matching angle. The existence of a phase matching direction in this material was confirmed by determining the variation of SH intensity with particle size [21]. The crystal having particle sizes in the range of <125 μm, 125–250 μm, 250–355 μm, and >355 μm were obtained using standard sieves of 125, 250 and 355 μm, respectively. The SH intensity was measured for all range of particle sizes with fixed laser input energy (0.27 mJ) and the resulting dependence of SH intensity on particle size is shown in Fig. 2. The SH intensity is independent of particle size if the particle size is higher than coherence length, l_c, of crystal. But, in non-phase matchable crystals, for a particle size greater than l_c, the SH intensity varies inversely with particle size, and hence a decrease of SH intensity was observed for particle size greater than l_c. From the Fig. 2, it is clear that the SH intensity increases with increasing particle size and attains saturation above the range of particle sizes 250–355 μm. Such results are observed only for phase matchable materials, such as CDBA [3], p-methoxy dibenzylideneacetone (PDBA) [4, 5], N-(3-nitrophenyl)phthalimide (NNPP) [24], and ammonium dihydrogen phosphate (ADP) [21]. Therefore, the existence of phase matching direction and also its high SHG efficiency suggests that this co-crystal is a promising material for second order NLO applications.

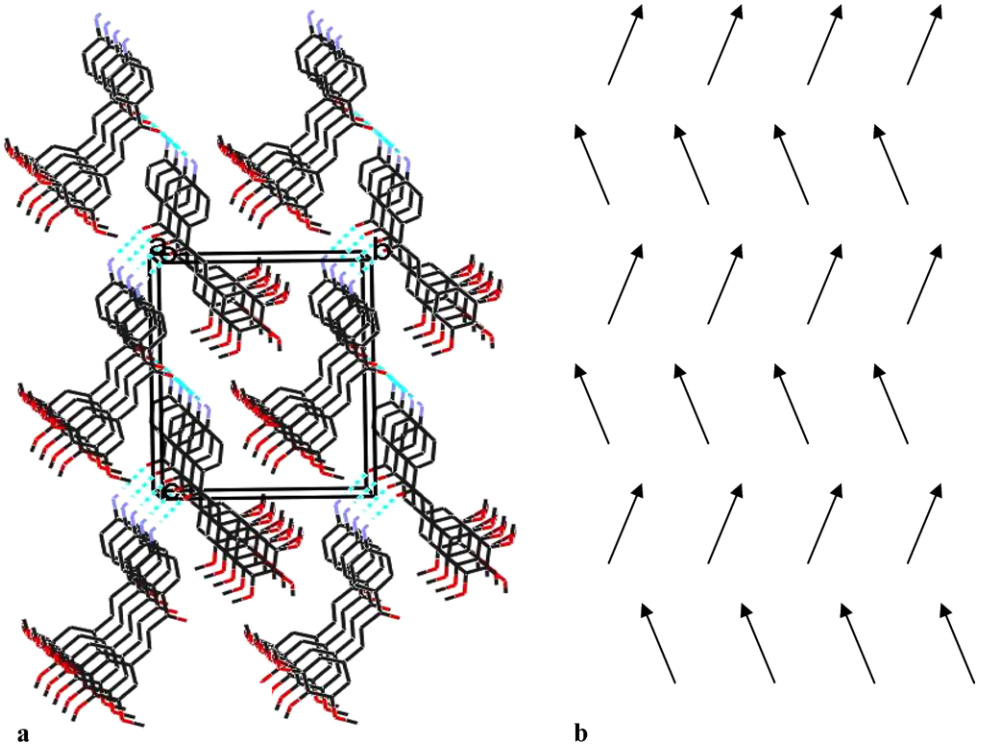

Fig. 2 **a** A crystal packing diagram of the co-crystal as viewed down the *a*-axis. The *dashed lines* represents the hydrogen bond interactions (all the hydrogen atoms are omitted for clarity except those atoms involved in hydrogen bond formation). **b** Head-to-tail alignment of molecular dipoles along the crystallographic *c*-direction

Chalcones are cross-conjugated molecules, and the carbonyl group in these systems breaks the conjugation system into two independent parts to have a two dimensional β character. The amino group attached to the benzoyl group in this chalcone is a strong electron donor and the three methoxy groups attached at the 3, 4, and 5 positions on the other phenyl ring also releases the electron to the π-conjugated system. The carbonyl (C=O) group at the middle acts as an electron acceptor and thus creates a donor–π–acceptor–π–donor (D–π–A–π–D) type structure, where the charge transfer is assumed to be from the ends to the center of the molecule. However, the electron donating ability of the amino group dominates over the methoxy groups at the other end of the chalcone, and the dipole moment vector of this molecule is more likely to be in the direction of carbonyl to amino group, which was regarded as the molecular charge transfer axis in this chalcone. The bromo substituted chalcone component (APBDP) may have a lower ground state dipole moment, as observed earlier with bromine substituted chalcones which resulted in noncentrosymmetric structures, and exhibits high SHG efficiency [23]. Therefore, the presence of bromine substituted component of chalcone in this co-crystal may contribute partly to the NLO properties.

The hydrogen bond interactions play a significant role in improving the SHG. It is observed that in crystals, such as MMONS and NMBA, the aromatic π–π stacking and hydrogen bond interactions (C–H$\cdots$X where X = N, O or π) help to create a delicate balance between the molecular and supramolecular charge transfer processes by creating

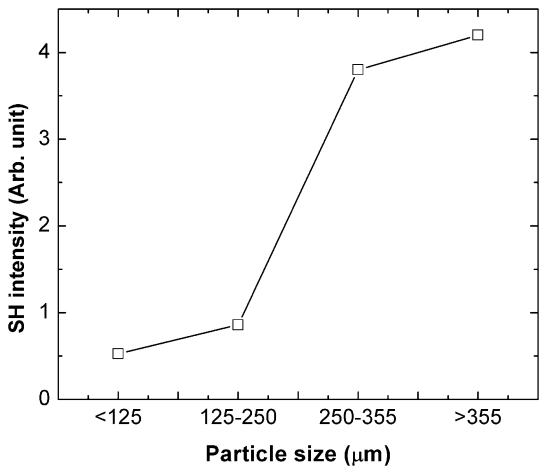

Fig. 3 Particle size dependence of SH intensity of the co-crystal

a noncentrosymmetric structure [25, 26]. Similarly, in this chalcone crystal structure, a weak N–H$\cdots$O hydrogen bond helps molecules to pack in a head–tail fashion along the crystallographic *c*-axis (Fig. 3). As a result, the dipole moment of each molecule adds to establish a net macroscopic polarization in this crystal. Even though the N–H$\cdots$O interactions are weak in this crystal, they may play a significant role in the exited state to extend the molecular charge transfer through intermolecular interaction into the supramolecular realm.

Due to the lack of crystal quality and size of the single crystal grown, the determination of the individual second-

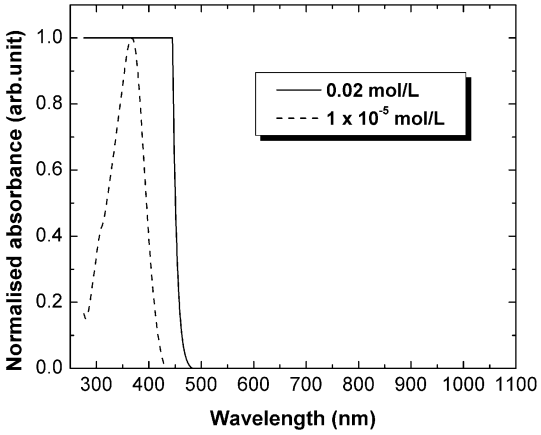

Fig. 4 UV–visible spectra of the chalcone dissolved in DMF solvent

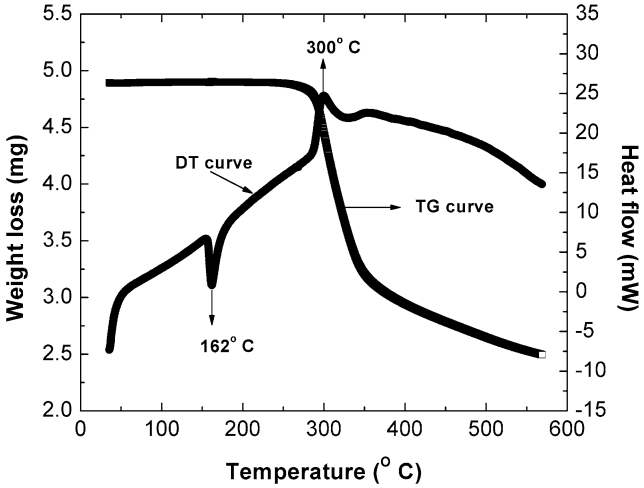

Fig. 5 TG/DT response curve of the chalcone co-crystal

order NLO d-coefficients of this crystal is not possible at present. However, based on the crystal structure and the molecular nonlinear optical susceptibility tensor, the nonlinear optical d-coefficients can be calculated from the relations [27] $d_{33} = N\beta f_3^2(\omega) f_3(2\omega) \sin^3(\theta)$ and $d_{32} = N\beta f_2^2(\omega) f_3(2\omega) \sin(\theta) \cos^2(\theta)$, where N is the number of molecules per unit volume, β is the molecular hyperpolarizability, $f_i(\omega) = [(n_i^2(\omega) + 2)/3]$ is the local field correction, and θ_c and θ_b are the angle between the molecular charge transfer axis and the crystallographic c-axis and b-axis, respectively. The values $\theta_c \approx 8°$ and $\theta_b \approx 82.4°$ were obtained from the crystal structure. The value of β was calculated using MOPAC2007 software [28]. The PM6 [29] optimized geometry was used for the first hyperpolarizability (β) calculation of this chalcone. The geometry was optimized using Eigenvector Following (EF) geometry optimizer and the molecular hyperpolarizability was computed using the Time-Dependent Hartree–Fock (TDHF) theory, and β was calculated to be 17.3×10^{-30} esu. The values of d_{33} and d_{32} were calculated to be 0.22 pm/V and 1.06 pm/V, respectively. Here we note that even though the intermolecular hydrogen bond interactions are weak, the way in which they link the molecules in the three dimensional lattice of the crystal makes a significant contribution to the NLO property and are not taken into account in this calculation.

For an effective use of any NLO crystal, a good transparency extending down to ultra-violet region and high laser damage resistance to use them in high power laser operation are essential. The UV–visible absorption spectrum was collected in the range of 250 to 1000 nm using Shimadzu UV-2450 spectrophotometer and the absorption spectrum is shown in Fig. 4. The maximum absorption corresponding to the wavelength 366 nm (λ_{max}) was observed for a very dilute solution (1×10^{-5} mol/l) of chalcone dissolved in DMF and assigned to an n–π^* transition, and may be attributed to the excitation in the aromatic ring and C=O group. The absorption spectra collected at higher concentration of the co-crystal dissolved in DMF as well as for a co-crystal of 1 mm thickness show a red shift in cut-off wavelength (470 nm) due to the increased linear absorption. The UV transparency was red-shifted compared to other chalcones, such as CDBA [3] and PDBA [5], due to the presence of more electron-donor methoxy groups and a strong electron-donor amino group.

The laser damage threshold of the co-crystal was determined using 8-ns pulses at 532 nm. The laser light was focused to a spot size of 20 μm using a lens of focal length 25 cm. The on-axis irradiance was increased in a step of 0.2 GW/cm^2, and the surface damage was observed under a microscope after delivering 10 pulses on the crystal in the single-shot mode. The laser damage threshold value of this crystal was found to be greater than 1.5 GW cm^{-2}, and is even higher in crystals having less linear absorption. The damage on the crystal could be due to the heating effect caused by linear absorption, and consequently the lower damage threshold was observed for the crystal having high linear absorption at 532 nm. The laser damage threshold of this crystal is better than the damage thresholds of reported NLO materials CDBA (0.6 GW cm^{-2}) [3] and urea (0.158 GW cm^{-2}) [30].

To check the thermal stability of the co-crystal, thermal analysis was carried out using a Perkin Elmer simultaneous TG/DT analyzer. The sample was scanned in the temperature range of 30–600°C in a nitrogen atmosphere with a heating rate of 5°C min^{-1}. The endothermic peak observed at 162°C (Fig. 5) corresponds to the melting point, and no weight loss was observed at this endotherm in the TG curve. The weight loss starts at 275°C, and the major weight loss was observed at 310°C and was attributed to decomposition. This co-crystal has significantly better thermal stability than other NLO chalcones reported in the literature [23] and also in comparison with urea (decomp. = 130°C) and PDBA (131°C) [5].

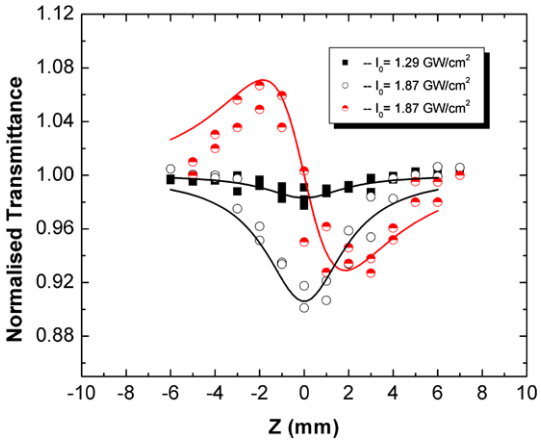

Fig. 6 Open and closed aperture Z-scan data of cocrystal solutions of DMF. **a** The open aperture Z-scan data represented by *filled squares* and *open circles* obtained at $I_0 = 1.29$ GW/cm^2 and $I_0 = 1.87$ GW/cm^2, respectively, and the *solid line* is the fit to the experimental data with $\beta_{\text{eff}} = 0.5$ cm/GW and $\beta_{\text{eff}} = 1.43$ cm/GW, respectively, using (1). **b** The *half filled circles* represent the pure nonlinear refraction data obtained by the division method, and the *solid line* is the theoretical fit

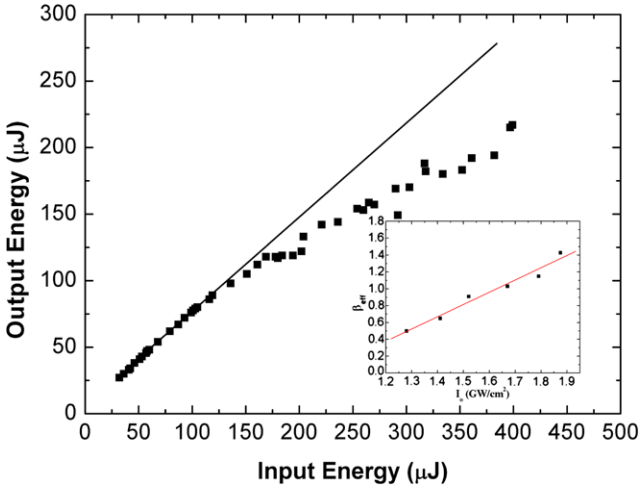

Fig. 7 Optical limiting of solutions of the chalcone co-crystal

5 Third order NLO properties

The measurement of third order nonlinearity of single crystals of this compound was not possible due to the lack of crystal quality and sufficient size. Therefore, we investigated the TNLO properties of this compound in solutions of DMF. The concentration used was 0.02 mol l^{-1}. The laser pulse energy was chosen so that the contribution from the solvent to the nonlinear refraction and absorption of solute was negligible. The closed and open aperture Z-scan measurements were carried out on pure DMF taken in a 1-mm quartz cuvette at the energy of 80 μJ to determine the contribution of solvent to the nonlinear abortion and refraction of this sample solution. The pure solvent does not show nonlinear absorption and refraction, and it can be concluded that the values obtained are due to the chalcone present in the solution.

For a temporal Gaussian pulse with an incident Gaussian spatial profile, the on-axis transmission has been shown as a function of sample position relative to the lens focal point and the normalized transmittance for the open aperture Z-scan is given by

$$T(z) = 1 - \frac{\beta I_0 L_{\text{eff}}}{2\sqrt{2}} \frac{1}{(1 + z^2/z_0^2)}, \tag{1}$$

where I_0 is the peak irradiance at the focus, β is the nonlinear absorption coefficient, z_0 is the Rayleigh length given by the formula $z_0 = k\omega_0^2/2$ with k being the wave vector and ω_0 the beam waist radius at the focus, and L_{eff} is the effective sample length.

The open aperture Z-scan data of the sample are shown in Fig. 6 along with the nonlinear refraction data obtained by dividing the closed aperture Z-scan data by the open aperture data. The nonlinear absorption coefficient was determined by fitting the experimental open aperture Z-scan data with (1). Similarly, the nonlinear refractive index was obtained by fitting the closed aperture Z-scan experimental data with the equation given in [22]. The n_2, β_{eff}, Im χ^3, and Re χ^3 at 80 μJ were found to be -0.54×10^{-11} esu, 1.43 cm GW^{-1}, -0.22×10^{-13} esu, and -0.583×10^{-13} esu, respectively. The molecular hyperpolarizability of this chalcone calculated using the formula $\gamma_{\text{h}} = \chi_R^{(3)}/L^4N$, where L is the local field factor and N is the number of molecules per cubic centimeter, was 0.203×10^{-32} esu. The femtosecond laser pulse Z-scan experiments on this chalcone [31] showed a self-focusing effect, indicating that the thermal effect did play a significant role in the ns Z-scan measurements, as was observed in the present study. The optical limiting behavior of this compound solution is shown in Fig. 7. The inset of the figure shows the variation of β_{eff} with the laser pulse energy. The β_{eff} increases with the increase in laser pulse energy, indicating the contributions from higher order nonlinear absorption (ESA) term to the β_{eff}. Materials that exhibit RSA usually shows good optical limiting characteristics of the high intensity laser pulses. In order to observe RSA, the exited state absorption cross-section should be higher than that of the ground state absorption cross-section and is consistent with the present result. Therefore, in this chalcone, the two-photon assisted exited state absorption leading to RSA may be responsible for the optical limiting action [31].

The molecular hyperpolarizability γ_{h} value of this compound was compared with those of chalcones reported in literature. It is found that the value of γ_{h} for this chalcone is greater than that of 4′-methoxy chalcone and chlorine substituted 4′-methoxy chalcone, and less than methoxy group substituted 4′-methoxy chalcone [32]. The decrease of γ_{h}

in this chalcone can be attributed to the experimental condition involved, and moreover the impurity APBDP may play a negative role, and hence resulted in low response. Recently, Gu et al. [31] reported the ultra fast NLO properties of APTP, and the value of γ_h reported by them was 5.79×10^{-33} esu, which is higher than the value reported here. The increase in hyperpolarizability value of APTP may be due to the higher concentration of the solute they used and also may be due to the solvent effect. They attribute the enhancement of TNLO property in this chalcone to the electron withdrawing nature of the amino group, but, in fact, the amino group is actually regarded as a strong electron donor [33].

In order to give the evidence for the electron donating nature of the amino group in these chalcones and to also understand the discrepancy in the decrease of the γ_h value of present compound compared to the γ_h values of methoxy substituted 4′-methoxy chalcone (9.19×10^{-33} esu), a systematic study of static second hyperpolarizability γ_0 was carried out using the MOPAC2007 computer program [28]. The calculations were performed using a PM6 Hamiltonian [29]. All the geometries of these molecules were optimized using the EF geometry optimizer where the geometry obtained from the single crystal X-ray diffraction study was used as the starting geometry. To calculate the static molecular second hyperpolarizability γ_0 of these molecules, Time-Dependent Hartree–Fock (TDHF) theory was used. The "PRECISE" keyword was used as a convergence criterion for PM6 calculation of geometries and the NLO properties. In order to understand the nature of charge transfer in these molecules, we optimized the first exited state geometry of these chalcones.

The static second hyperpolarizability, $\gamma_{0,}$ for all the chalcone derivatives and APTP are tabulated in Table 2. The charge on the carbonyl carbon atom for all the chalcones is listed for both ground and exited state in Table 2. We have computed γ_0 for seven chalcone molecules including the present compound APTP to study (i) the effect of the strength of the electron donor group substitution at the R_1 position of the chalcone on the molecular hyperpolarizability; (ii) the electron donating nature of the amino group, and (iii) the effect of multiple methoxy groups substitution at the R_2, R_3 and R_4 positions of the phenylene group.

In compounds 1, 3, and 4, the substituents at the R_1 position of the benzoyl ring were varied by substituting the electron donor group with increasing electron donating strength, i.e., with H, OCH_3 and NH_2, respectively, where one OCH_3 group was fixed at the R_3 position of the phenylene group. Thus, the variation of the NLO response depends only on the type of the substituent at R_1. The increase of γ_0 value from compound 1 to 4 clearly indicates the strong electron donating nature of the NH_2 group. However, the γ_0 value obtained for compound 2 is higher compared to that for compound 4, which indicates that the substitution of an electron withdrawing group is much more effective compared to a strong electron donating group at R_1 position of chalcones. For instance, the charges on the carbonyl (C=O) carbon atom in compounds 1–4 are 0.557722, 0.557722, 0.580043, and 0.58283, respectively, and those for the excited state are 0.486182, 0.484081, 0.511203, and 0.509634, respectively. The increase of charge on the carbonyl carbon atom is more prominent when R_1 is substituted with an electron withdrawing group Cl in compound 2, indicating that charges are pulled towards the electron withdrawing group, the carbonyl group. Due to the competition between the electron-donating abilities of the donor groups substituted at either end of the molecule, the effective charge transfer is affected by pushing the electron from the one end of the molecule to other. The substitution of a strong electron donor group at the R_3 position is much more effective [33], and to have the best result with a strong donor at R_3, a relatively weak donor or a strong electron withdrawing group at R_1 position was found to be more effective in enhancing the hyperpolarizabilities in the chalcone molecules [33]. But in compound 5, the γ_0 decreased compared to compound 4. The decrease in γ_0 is attributed to the steric hindrance caused by the multiple bulky methoxy groups present at the R_2, R_3 and R_4 positions which affect the intramolecular charge transfer. Moreover, the substitution of strong donors at both ends also affects the effective charge transfer due to the competition between the donating ability of electron donor groups. It is clear from the solid state structure reported for trimethoxy substituted chalcones [16–19] that the methoxy group attached at the R_3 position is pushed out of plane due to the presence of two more adjacent bulky methoxy groups in the benzene ring. For an effective charge transfer, a planarity of the molecule is essential, and therefore, though there are three methoxy groups, they hardly contribute to the NLO property due to the steric effect.

Further, the three methoxy groups were fixed at R_2, R_3 and R_4 positions of the phenylene group, and the strength of the donor was increased by substituting with Cl, OCH_3 and NH_2 at R_1. As expected, the strength of the donor at R_1 was responsible for an increase of γ_0 value from compound $7 \rightarrow 5$. The amino group substituted in compound 5 showed higher nonlinear response than the methoxy and Cl substituted ones (compounds 6 and 7). The decrease in charge on the carbonyl carbon in compound 6 was larger compared to the one substituted with the amino group, suggesting that the strong donor at R_1 is not effective, but the γ_0 of compound 5 was almost the same as that of compound 6. The reason for the decreased γ_0 value obtained in the Z-scan study may be attributed to the ineffective charge transfer that lead to a decrease of the NLO property of the solution.

Therefore, we conclude from the above results that (i) a stronger donor substitution at R_3 is more effective than substitution at R_1; (ii) increasing the number of donor groups at

Table 2 Calculated hyperpolarizabilities of chalcones

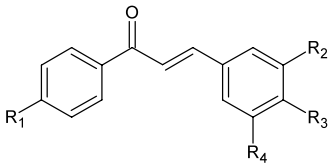

	R_1	R_2	R_3	R_4	$\gamma_0(\times 10^{-36}$ esu)	Charge on the carbonyl carbon	
						Ground state	Excited state
1	H	H	OCH_3	H	47.7	0.557722	0.486182
2	Cl	H	OCH_3	H	59.4	0.563435	0.484081
3	OCH_3	H	OCH_3	H	56.9	0.580043	0.511203
4	NH_2	H	OCH_3	H	58.7	0.582833	0.509634
5	NH_2	OCH_3	OCH_3	OCH_3	49.2	0.575052	0.501505
6	OCH_3	OCH_3	OCH_3	OCH_3	47.9	0.573066	0.452713
7	Cl	OCH_3	OCH_3	OCH_3	44.1	0.552984	0.541015

R_2, R_3 and R_4 is not suitable, and instead a single donor at the R_3 position is the most effective, and (iii) a strong electron donor at R_3 and a weak electron donor or a strong electron withdrawing group at R_1 is much more effective than having donors with equal donating ability at the R_1 and R_3 positions in these chalcones. The results clearly show that the amino group is a strong electron donor, and therefore the NLO response in the present compound can be attributed to the electron donating character of the amino group.

6 Conclusions

Single crystals of the chalcone co-crystal (APTP/APBDP) were grown by slow solution evaporation growth technique. The crystals were characterized by spectroscopic and single crystal X-ray diffraction techniques. The high SHG and phase matching property of this chalcone came from the head-to-tail alignment of molecules facilitated through N–H···O hydrogen bond interactions. The good transparency, thermal stability, high laser damage threshold, and high SHG in this chalcone co-crystal indicate that it is a promising material for frequency doubling applications. The molecule shows good third order NLO properties and exhibits a self defocusing effect of 8 ns laser pulses at 532 nm. The optical limiting may be attributed to reverse saturable absorption. For a better NLO response in chalcones, a substitution of a strong electron donor group at the phenylene group was found to more effective rather than at the benzoyl group. Increasing the number of donor methoxy groups at the phenylene group was unnecessary, and a single methoxy group plays a much more effective role in enhancing NLO properties.

Acknowledgements The authors thank Prof. P.K. Das, IISC, Bangalore and Prof. B. Timmegowda, Department of Chemistry, Mangalore University for providing experimental facilities, Mr. Sharafudeen for his help. H.J.R thanks DAE-BRNS for the project fellowship. S.M.D thanks DST for the research project grant (No. SR/S2/LOP-17/2006).The authors thank Dr. John Kiran for his fruitful discussions and suggestions.

References

1. J. Zyss, *Molecular Nonlinear Optics: Materials, Physics and Devices* (Academic Press, Boston, 1994)
2. R.W. Munn, C.N. Ironside, *Principles and Applications of Nonlinear Optical Materials* (Chapman & Hall, London, 1993)
3. H.J. Ravindra, A.J. Kiran, R.N. Satheesh, S.M. Dharmaprakash, K. Chandrasekharan, K. Balakrishna, F. Rotermund, J. Cryst. Growth **310**, 2543 (2008)
4. A.J. Kiran, H.C. Kim, K. Kim, F. Rotermund, H.J. Ravindra, S.M. Dharmaprakash, H. Lim, Appl. Phys. Lett. **92**, 113307 (2008)
5. H.J. Ravindra, A.J. Kiran, R.N. Satheesh, S.M. Dharmaprakash, K. Chandrasekharan, K. Balakrishna, F. Rotermund, J. Cryst. Growth **310**, 4169 (2008)
6. T. Uchida, K. Kozawa, T. Sakai, M. Aoki, H. Yoguchi, A. Abduryim, Y. Watanabe, Mol. Cryst. Liq. Cryst. **315**, 135 (1998)
7. P. Vishweshwar, J.A. McMahon, M.L. Peterson, M.B. Hickey, T.R. Shattock, M.J. Zaworotko, Chem. Commun. **12**, 4601 (2005)
8. B.K. Saha, A. Nangia, M. Jaskolski, Cryst. Eng. Commun. **7**, 355 (2005)
9. T. Friscic, L.R. MacGillivray, Chem. Commun. 1306 (2003)
10. A.V. Trask, W.D.S. Motherwell, W. Jones, Cryst. Growth Des. **5**, 1013 (2005)
11. A.N. Sokolov, T. Friscic', L.R. MacGillivray, J. Am. Chem. Soc. **35**, 3523 (2006)
12. M.D. Hollingsworth, Science **295**, 2410 (2002)
13. A.V. Trask, W. Jones, Top. Curr. Chem. **254**, 41 (2005)
14. F. Toda, Chem. Rev. **100**, 1025 (2000)
15. D. Braga, S.L. Giaffreda, F. Grepioni, A. Pettersen, L. Maini, M. Curzi, M. Polito, Dalton Trans. **12**, 1249 (2006)
16. H.J. Ravindra, S.M. Dharmaprakash, W.T.A. Harrison, Acta Cryst. E **63**, o2877 (2007)
17. S.-L. Ng, I.A. Razak, H.-K. Fun, P.S. Patil, S.M. Dharmaprakash, Acta Cryst. E **62**, o4650 (2006)
18. S.-L. Ng, P.S. Patil, I.A. Razak, H.-K. Fun, S.M. Dharmaprakash, Acta Cryst. E **62**, o1228 (2006)
19. W.T.A. Harrison, H.J. Ravindra, M.R.S. Kumar, S.M. Dharmaprakash, Acta Cryst. E **63**, o3970 (2007)

20. A.I. Vogel, in *Vogel's Textbook of Practical Organic Chemistry*, 5th edn., ed. by A.I. Vogel, B.S. Furniss, A.J. Hannaford, P.W.G. Smith, A.R. Tatchell (Longman Group, London, 1999)
21. S.K. Kurtz, T.T. Perry, J. Appl. Phys. **39**, 3798 (1968)
22. M. Sheik-Bahae, A.A. Said, T.-H. Wei, D.J. Hagan, E.W. Van Stryland, IEEE J. Quantum Electron. **QE-26**, 760 (1990)
23. B. Zhao, W.-Q. Lu, Z.-H. Zhou, Y. Wu, J. Mater. Chem. **10**, 1513 (2000)
24. H.J. Ravindra, M.R.S. Kumar, C. Rai, S.M. Dharmaprakash, J. Cryst. Growth **294**, 318 (2006)
25. J.M. Cole, J.A.K. Howard, G.J. McIntyre, Acta Cryst. B **57**, 410 (2001)
26. W. Tam, B. Guerin, J.C. Calabrese, S.H. Stevenson, Chem. Phys. Lett. **154**, 93 (1989)
27. J. Zyss, L. Oudar, Phys. Rev. A **26**, 2028 (1982)
28. J.J.P. Stewart, MOPAC2007, Stewart Computational Chemistry, Colorado Springs, CO, USA, 2007. http://OpenMOPAC.net
29. J.J.P. Stewart, J. Mol. Model. **13**, 1173 (2007)
30. G.C. Bhar, A.K. Chaudhary, P. Kumbhakar, Appl. Surf. Sci. **161**, 155 (2000)
31. B. Gu, W. Ji, P.S. Patil, S.M. Dharmaprakash, J. Appl. Phys. **103**, 103511 (2008)
32. H.J. Ravindra, A.J. Kiran, K. Chandrasekharan, H.D. Shashikala, S.M. Dharmaprakash, Appl. Phys. B: Lasers Opt. **88**, 105 (2007)
33. D. Wu, B. Zhao, Z. Zhou, J. Mol. Struct. **682**, 83 (2004)